Ballistic aggregation on two-dimensional arrays of seeds with oblique incident flux: Growth model for amorphous Si on Si

D.-X. Ye* and T.-M. Lu

Department of Physics, Applied Physics and Astronomy, Rensselaer Polytechnic Institute, Troy, New York 12180-3590, USA

(Received 5 June 2007; published 3 December 2007)

Amorphous silicon (Si) structures on two-dimensional arrays of seeds on a Si substrate were experimentally prepared at near room temperature using a physical vapor deposition system with an 85° oblique incident flux. In the stationary deposition case where the substrate is fixed at a position, the Si on the seeds form a ballistic inclined fanlike structure with an initial cone shape and the fan size R grows with time in a power law form t^p, where $p \sim 1$. We show that with a swing rotation where the substrate is rotated back-and-forth azimuthally, the fan size grows slower ($p<1$) relative to that of the stationary deposition case and then saturates at a size depending on the swing angle. We proposed a modified ballistic deposition model considering the ballistic sticking, shadowing, surface diffusion, and substrate rotation in a three-dimensional Monte Carlo simulator. The evolution of the fanlike structures at different deposition times was simulated for both stationary deposition and swing rotation. The growth of the fan size R with time t in simulations was quantitatively analyzed and the exponents $p \sim 1.0$ and $p \sim 0.46$ were extracted for the stationary deposition and the swing rotation, respectively. For stationary deposition, the exponent 1 does not change significantly with the strength of surface diffusion. However, the fan-out angle decreases with the increased strength of surface diffusion. For swing rotation, the reduced exponent 0.46 at the initial stages of growth is primarily due to the self-shadowing of the fan itself under rotation. At the later stages of growth, the saturation of the fan size produces uniform rods and is due to the global shadowing from the adjacent fan structures. The morphology and the exponent obtained from our simulations are consistent with our experimental observations.

DOI: 10.1103/PhysRevB.76.235402 PACS number(s): 68.55.−a, 81.15.−z

I. INTRODUCTION

Nonequilibrium aggregation processes have been studied using theories and computer simulations for many decades: for example, the growth of bacterial colonies, the aggregation of snowflakes, and atom deposition on a surface.[1–3] The essential characteristics of these nonequilibrium aggregations are the irreversible accumulation of particles and the inherently nonlocal nature of the process. As a result, aggregations with intriguing geometry can be formed in a manner of self-organizing under a highly nonequilibrium condition. Thus far there are two basic models, diffusion-limited aggregation (DLA)[4] and ballistic aggregation (BA),[5] introduced to study the abovementioned processes. In the DLA model, one particle or a cluster of particles is launched far from a seed and approaches the seed under the Brownian motion until it arrives at a site adjacent to the aggregate. Then, another particle with a random position is launched and diffused towards the aggregate, and so forth. In contrast, in the BA process, the randomly launched single particles or clusters of particles move along straight trajectories towards a seed one at a time from all directions. Computer simulations and experiments have demonstrated that the structures generated by a DLA process possess fractal dimensions;[3,4] however, the structures formed by BA are typically not fractals.[6–9]

A simplified version of BA considers the trajectory of the incoming particles to be parallel.[9–14] A particle will stick to the surface of the structure when it comes close to a previously added particle in the growing aggregate. This aggregation results in the formation of a fanlike structure if the initial seed is a structureless point.[11] This simplified BA model can be useful for the study of surface growth processes, such as physical vapor deposition on a cold substrate under high vacuum. As the pressure inside the deposition system is low, the mean free path of the particles can be long enough such that the collisions between two particles is negligible before they hit the substrate. The trajectory of the particles under this condition can certainly be treated as a straight line. Giving the geometry of the deposition system, specifically, the distance between the source and the substrate, and the size of the substrate, the lines of flight may be parallel to each other.[15]

It has been shown by theoretical analysis and computer simulations that the initial seeds determine the morphology of ballistic aggregates with parallel moving particles. The evolution of the morphology follows different nontrivial growth behaviors starting from different types of seeds as well. If the initial seed is a point, the resulting aggregate demonstrates a fanlike structure with the width of the fan R growing linearly with deposition time t, that is,

$$R \sim t^p, \tag{1}$$

where $p=1$ is the exponent of the growth.[11,12,16] From computer simulations, the cumulation of aggregates is independent of the size of the initial seeds with parallel flux.[13] Ramanlal and Sander furthermore predicted a cosine profile of the ballistic fan's top surface in their two-dimensional mean field theory[11]

$$H(\phi) = H_0\sqrt{\cos\phi}, \quad (0 \le \phi \le \pi/2), \tag{2}$$

where H_0 is a time-dependent parameter and ϕ is the polar angle measured from the axis of the fan. We experimentally demonstrated recently that Eq. (2) can be used as the first

order approximation of the top-surface profile of our fanlike structures grown on seeds under normally incident deposition flux.[16]

In the case of oblique angle deposition without substrate motion, the growing features tend to incline toward the incident flux to a tilted angle β, which is measured from the substrate normal. It is distinctive that this tilt angle is less than the angle of incidence of the deposition flux θ. There is an empirical rule known as the "tangent rule" describing the relation of β and θ as [17,18]

$$\tan \beta \approx (1/2)\tan \theta. \tag{3}$$

The origin of the tangent rule is generally believed to be due to the limited surface diffusion and the shadowing of atoms on the surface.[19] Dirks and Leamy obtained Eq. (3) from computer simulations, based on the assumptions that atoms have finite size and that the shadowing of atoms deposited in the neighboring area affects the growth.[20] This tangent rule is not universal however because the tilted angles of the nanostructures also depend on the deposition conditions and the material properties.[21–23] Even for the same material, the tangent rule will not hold for all incident angles. For larger incident angles ($\theta > 60°$), another empirical rule called the "cosine rule" may give a better fit of the experimental data.[24,25] The cosine rule can be written as

$$\beta = \theta - \arcsin\left(\frac{1-\cos\theta}{2}\right). \tag{4}$$

In this paper, we designed a planar surface (substrate) containing arrays of seeds to study the BA with oblique incident flux from both experiments and Monte Carlo simulations. When the substrate is held at a position with the incident angle $\theta = 85°$, a fanlike structure is formed on each seed with the axis of the structures tilting toward the source of the particles. The axis of the fan inclines towards the source with an angle β, which can be related to the incident angle θ by Eq. (4). We observed a linear growth behavior of the width of the fanlike structure in the direction perpendicular to the flux; that is, the growth exponent in this direction equals 1. If the deposition time is long enough, the fanlike structures connect their neighbors along the direction perpendicular to the flux. As a result, there are no more isolated individual fanlike structures deposited on the seeds. We also rotated the substrate back-and-forth to a limited azimuthal angle and observed that the growth exponent p is changed to about 0.46 by this rotation. From our Monte Carlo simulations, we observed that this growth exponent ($p \sim 0.46$) is mainly due to the self-shadowing effect by the individual fan itself. Each of the fans reaches a maximum width and becomes a uniform-size rodlike structure due to the global shadowing effects from adjacent fans.

II. EXPERIMENTAL SETUP AND MONTE CARLO SIMULATIONS

Silicon (Si) source and substrate holder were housed in a high vacuum thermal evaporation system schematically represented by Fig. 1(a). Si of 99.9999% purity was evaporated

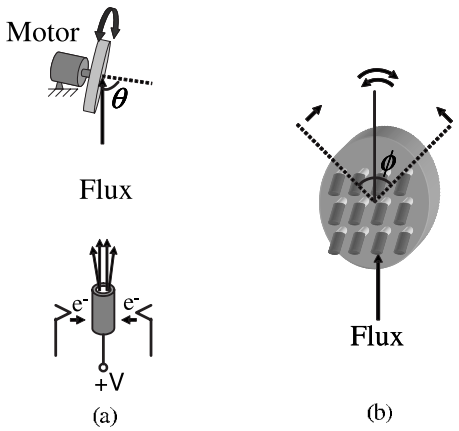

FIG. 1. Schematics of (a) the oblique angle deposition system with a flux incident angle θ and substrate rotation by a motor and (b) the "swing" substrate rotation method. ϕ is the swing angle.

out of a cylindrical graphite crucible by an electron bombardment method described previously.[26] The crucible has a diameter of 1 cm at the opening. The system was maintained at a total pressure of less than 4×10^{-4} Pa during the experiment using a diffusion pump. The chamber wall was cooled by 4 °C circulating water. We used prefabricated tungsten pillars on Si substrates as the aggregation seeds that have been described in details elsewhere.[16] The cylindrical shape pillars (seeds) have a diameter of about 150 nm and a height of about 220 nm. The total area containing the seeds is about 0.5 cm^2. The seeds were arranged in a square lattice with a 1000 nm lattice constant. The substrates were mounted on a stepper motor above the Si source with a distance as large as 35 cm measured from the opening of the crucible. With the geometry of the deposition system, the mean free path of Si particles is much larger than the dimension of the system. Therefore, the Si flux approaching the substrate is ballistic and uniform with less than 2° angular spread of the flux. The stepper motor was adjusted to a position allowing an incident angle of the depositing flux $\theta = 85°$, respective to the normal direction of the substrate, as schematically shown in Fig. 1(a). The back-and-forth motion of the substrate, as shown in Fig. 1(b), can be driven by the stepper motor through a computer program. The rotational speed of the substrate was set to 0.27 revolution per minute (rpm). This type of growth mode, to which we refer as "swing rotation," has been described in details by our previous paper.[27] The evaporation rate and the normal thickness of Si were measured by a quartz-crystal microbalance (QCM, TM-400, Maxtek Inc., USA). The evaporation rate was 30±2 nm/min during the deposition. Si films were deposited at near room temperature (the substrate temperature was less than 80 °C during the deposition). After depositions, the films were characterized by a field emission scanning electron microscope (SEM) system (FESEM-6350, Jeol, Ltd., Tokyo, Japan).

We performed 3D Monte Carlo simulations to mimic the formation of fanlike structures by shadowing effects under oblique angle incident flux. This 3D Monte Carlo simulation was based on a simple cubic lattice with the size of $1024 \times 1024 \times 1024$, and a periodic boundary condition was em-

ployed. Preoccupied sites in a square pattern on the x-y plane were designed to serve as the seeds. The particles which are cubes with one unit size approach the system one at a time at a given oblique angle $\theta=85°$, measured from the z direction, until they are deposited on the surface, or trapped by their nearest neighbors along the trajectory. The particle was generated at a random position on the x-y plane and one unit higher than the maximum height of the deposited structures in the z direction. The particle approached the surface in a stepwise manner. The next step was randomly selected from a group of possible positions; but the overall trajectory was determined by the preset incident angle θ. When the program had determined the next step of the moving particles, it checked if that lattice point was occupied or not. Unlike the traditional BA simulations, we allowed the deposited particles to diffuse. That is, after a particle was deposited, one particle (which could be the newly added particle itself) within a certain distance was activated to diffuse into a nearby empty site if the move can increase the number of neighboring bonds. The diffusion was repeated until reaching a limiting number D/F, where D is the number of candidate particles for diffusion while F is the number of particles added into the system during the same time interval. F equals 1 in our simulation scheme because the particles were sent one at a time. This parameter D/Fcan be treated as the diffusion strength of the materials. We set $D/F=100$ $(F=1)$ in the simulation of Si fanlike structures, according to our previous work.[16] The direction of the trajectory was fixed on the x-y plane for the stationary deposition at oblique angle incidence. However, this direction was continuously changed on the x-y plane within an angular range to mimic the "swing rotation" mode of the oblique angle deposition. After a certain number of particles were deposited, snap shots of the aggregates were generated using the simulation code to form the top view and cross-sectional view of the structures. The width of the aggregates on each seed was measured from the top view using the ADOBE® PHOTOSHOP® software (version 6.0, Adobe Systems, Inc., California, USA).

III. RESULTS AND DISCUSSION

The aggregated structures in our simulations were compared to our experimental data. The growth exponents of BA were obtained from the simulations for the "stationary deposition" and the "swing rotation" cases.

A. Ballistic aggregation on fixed substrates

1. Experimental results

Experimentally, we observed that the growth on a templated substrate with a regular array of seeds [see Fig. 2(a)] would give rise to a phenomenon which we now call "fan-out" growth in oblique angle deposition without substrate rotation. Figures 2(b) and 2(c) demonstrate this phenomenon by the SEM top-view image and cross-sectional image of the deposition on the seeds arranged in a square lattice, respectively. Si was deposited on the templated substrate with an 85° incidence angle. The normal thickness of the growth was 2000 nm as measured by the QCM. The specimens were

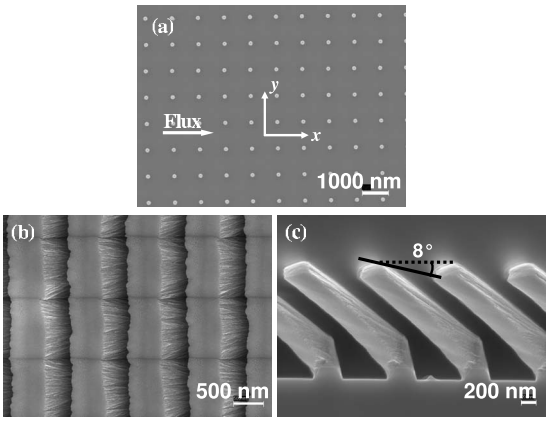

FIG. 2. "Fan-out" growth on tungsten pillars arranged in a square lattice at an oblique angle incidence $(\theta=85°)$ and under stationary substrate. (a) The SEM top-view image of the seeds (tungsten pillars) before deposition. (b) and (c) are the SEM top views and cross-sectional views of the final structures deposited on the seeds. The 8° measurement shown in (c) indicates the global shadowing by adjacent structures along the direction of the incident flux. The normal thickness of the deposition was 2000 nm.

tilted to 15° when taking the SEM cross-sectional images. In the "fan-out" growth, the size of the fanlike structures overgrows along the direction perpendicular to the incident deposition flux, which is along the y axis (or, y direction) as shown in Fig. 2(b). The result is that the size of the structures cannot be controlled as they grow. If the deposition time is long enough, the structures grown on the seeds will touch their neighbors from the side along the direction of the y axis. Thus, individual structures cannot be distinguished along this side. There is no shadowing effect in the y direction. However, the shadowing in the x direction is severe, as the substrate is fixed and the flux is aligned to the x direction. Due to the shadowing effect, the gap between the seeds along the x direction is still maintained even with the merging of structures in the y direction.

Figure 2(c) shows that the Si structures on the seeds were inclined toward the source at an angle of $\beta=52.3\pm0.3°$ measured from the normal of the substrate. Ten individual Si structures were selected for the measurement of the tilted angle β from the cross-sectional SEM images. Since the incident angle θ is very large, this tilted angle β can be predicted to be about 57.8° using Eq. (4). In contrast, the conventional tangent rule predicts an ~80° tilted angle with the incident angle $\theta=85°$ using Eq. (3). The size of the structures along on the x direction remained roughly constant at 340.3 ± 6.0 nm for the rods grown on the square lattice seeds. The top-end surface was found to be not exactly parallel to the x-y plane but with a slight tilt of ~8° from this plane. We believe this result is due to the geometry of the shadowing effect along the x direction. We draw a line from the higher edge of this surface to the lower edge of the next surface of the structure along the flux direction and obtained an ~8° angle with respect to the horizontal dotted line, as shown in Fig. 2(c). The direction of line is along the direction of the incident flux. From the images shown in Figs. 2(b) and 2(c), it is clear that the top-end surface of the structures is

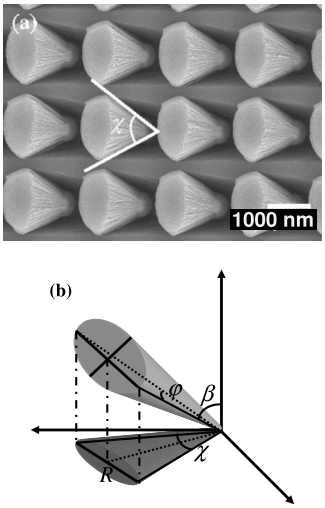

FIG. 3. (a) The SEM image of the "fan-out" growth at $\theta=85°$ and under stationary substrate before the structures merging in the y direction. The normal thickness of the deposition was 1000 nm. (b) The geometrical relationship between the projected "fan-out" angle χ and the real "fan-out" angle φ.

smoother than the surface on the sides. The face of the latter surfaces contains small fibers growing toward the source. This suggests that the structure may be constructed by the bundling of these small Si fibers.

Since the structures have touched each other in the y direction for a long deposition time, as shown in Figs. 2(b) and 2(c), no information about the initial stage of the growth can be obtained. Therefore, samples prepared using a sufficiently short deposition time were selected for the demonstration of the early stage of growth behavior of the fanlike structures. In Fig. 3, the normal thickness is about 1000 nm measured by the QCM. The structures deposited on the square lattice have been isolated without the merging in the y direction for this short deposition time.

First, we are interested in the characteristic angle of the fanlike Si structures as marked in Fig. 3(a). The angle χ can be measured from the SEM top-view images using the ADOBE® PHOTOSHOP® software. However, the SEM top-view images do not have any depth resolution. Therefore, the angle χ measured using PHOTOSHOP® is the projected fan-out angle in the x-y plane (also the plane of substrate). Since we know the tilted angle β of the structures from the cross-sectional views, we can convert this projected fan-out angle χ into a real fan-out angle φ using the following equation from the geometrical relationship shown in Fig. 3(b):

$$\varphi = 2 \arctan\left(\tan\left(\frac{1}{2}\chi\right)\sin\beta\right), \tag{5}$$

where β is the tilted angle of the structures. From the SEM images in Fig. 3(a), we measured the angle $\chi=60.6\pm0.4°$ on the square lattice and therefore $\varphi=49.6\pm0.5°$ from Eq. (5). Nonetheless, we used the projected fan-out angle χ to represent the fan-out angle of the fanlike structures in the following discussion.

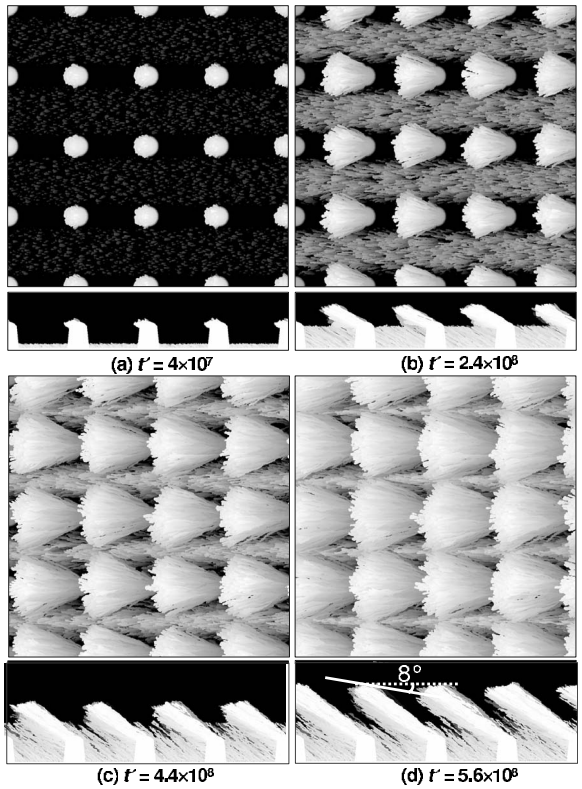

FIG. 4. Top view and cross-sectional view of fan-out growth at various simulation time t' under stationary substrate in the Monte Carlo simulations with nearest-neighbor sticking model. The particles were sent into the system from the left at an incident angle $\theta=85°$. The diffusion strength was set to $D/F=100$.

Secondly, we noticed that the enveloping surface appeared to have a cone shape. This indicates that the width R of the fanlike structures grows linearly with deposition time when measured in the y direction. In the other words, the exponent $p=1$ in Eq. (1). The result will be interesting because the exponent has been determined to be 1 in BA with normally incident flux on seeds without a shadowing effect from adjacent aggregates from our previous work.[16] Therefore, the exponent $p=1$ may define a growth universality. The width of the structures in the x direction is much uniform, suggesting a very small exponent due to the shadowing effect in this direction.

2. Monte Carlo simulation results

Monto Carlo simulations were used to quantitatively study the dynamic growth of the fanlike structures with varying deposition time. The system size was $1024\times1024\times1024$ in our computer simulations. Cylindrical seeds with a diameter of 36 units were used in the simulations. The size of the seeds in simulation does not necessary represent the real size of the seeds in the experiment. The height of each seed was 80 units. The lattice constant was 256 units for the seeds arranged in a square lattice. The flux was uniformly incident at an angle $\theta=85°$ with respect to the normal of the surface. Figure 4 shows the top views and cross-sectional views generated at different times t' in the Monte Carlo simulations.

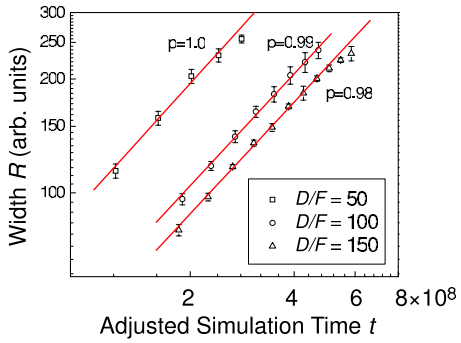

FIG. 5. (Color online) The simulated width R of the fan-out structures under stationary substrate in the y direction follows a power law in the form of $R \sim kt^p$. The simulation time t was adjusted to meet the boundary condition of $R=0$ at $t=0$. Three diffusion strengths ($D/F=50$, 100, and 150) were presented.

The simulation times t' are defined by the total number of particles sent into the simulation system. The upper images are top-view images and the bottom ones are cross-sectional images in four composite figures. The particles were deposited on the top area of individual seeds as well as the side wall of the seeds by nearest-neighbor (NN) sticking. A fanlike structure is formed by BA of particles. A film with random slanted nanorods was deposited inside the gaps between seeds. The diffusion strength in this simulation was set to $D/F=100$ ($F=1$) representing the diffusivity of the material such as Si.[16]

The width R of the fanlike structures was measured from the top view in the y direction and plotted in a logarithmic scale vs an adjusted simulation time t as shown in Fig. 5 following the method we introduced previously.[16] Basically, the simulation time t was adjusted to meet the boundary condition of $R=0$ at $t=0$. The exponent p determined from this plot is ~ 1, which confirmed the linear growth of the fanlike structures in the y direction. We tried other values of the diffusion strength D/F in simulations. The results show no significant difference from those simulated structures shown in Fig. 4. But the fan-out angles χ were found to be greatly dependent on the diffusion strength from our simulation results, as shown in Table I. We used the ADOBE® PHOTOSHOP® software to measure the angles following the same methods in analyzing the experimental data. The top views selected for the fan-out angle χ measurement are the images with a simulation time $t'=2.4\times 10^8$; and the figures selected for the tilted angle β measurement are those with the simulation time $t'=6.4\times 10^8$. In fact, the results of the tilted angles β do not have significant difference when measured at different simulation times. Nine individual structures were selected for the measurement of the fan-out angle χ. The average value was obtained from these nine measurements. The results of tilted angle β were also shown in Table I. From Table I, one can see that the tilted angles become larger as the diffusion becomes stronger; though the fan-out angles become smaller. The experimentally measured χ and β from Fig. 3 were also shown in the same table. From this table, we can identify that the set of data with $D/F=100$ is the closest one compared to the measured experimental results for the Si fans.

B. Ballistic aggregation on swinging substrates

1. Experimental results

The ability to uniformly grow isolated individual nanostructures is of considerable interest. However, the fanlike growth of structures would not be able to yield completely isolated and uniform nanostructures. As previous studies revealed, it is possible to create isolated nanostructures by using oblique angle deposition with delicate control of substrate motion.[27–30] Specifically, when the substrate is continuously rotated, vertical nanorods will be formed on the templated surface containing cylindrical seeds. If the substrate is rotated at a sufficient slow speed, 3D nanosprings can be created. The central axis of the spring is along the surface normal. The effect of substrate motion is equivalent to that of the rotation of the incident particle flux during deposition while keeping the substrate stationary.

There are two possible shadowing effects in the case of substrate motion: (a) self-shadowing effect due to the geometry of the growing structures[31] and (b) global shadowing effect from the structures grown on adjacent seeds when the substrate is moved to certain positions. In this paper, the term "self-shadowing" is used to describe the shadowing of one part of an individual structure by the part of the same structure exposed to the flux as the substrated is rotated, i.e., a pure geometric effect. Because of the NN sticking, the aggregate is allowed to grow not only in the direction along the incident flux but also in the direction perpendicular to the flux, leading to the linear fan-out growth (with growth exponent $p=1$) as discussed above. However, when the substrate is rotated during deposition, the growth velocity changes direction in an oscillating manner in the direction perpendicular to the incident flux. Therefore, the average growth velocity is slower in this direction due to the self-shadowing effect as compared to the no swinging case.

When swinging the substrate in our experiments, we have observed that the structures deposited on the seeds grow with

TABLE I. Extracted fan-out angles χ and tilted angles β for the structures formed in the Monte Carlo simulations with different diffusion strengths D/F. The particles were sent into the simulation system at a same direction with an oblique angle of incidence $\theta=85°$ under a stationary substrate. Experimental data measured from SEM images were listed on the right column.

D/F ($F=1$)	0	50	100	150	Experimental data
Fan-out angle χ (deg.)	107.2±2.4	94.7±2.1	62.0±2.0	50.8±1.4	60.6±0.4
Tilted angle β (deg.)	38.0±0.7	42.4±0.4	53.6±0.2	60.8±0.4	52.3±0.3

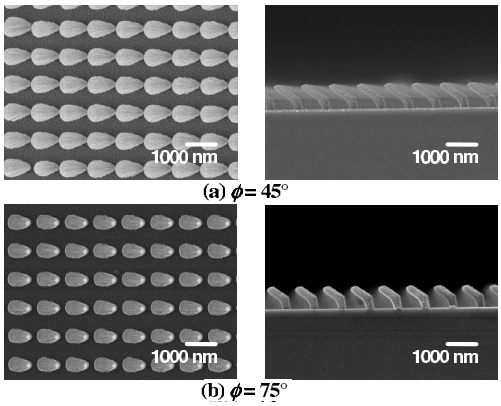

FIG. 6. SEM images of slanted Si structures grown on seeds (tungsten pillars) arranged in the square lattice by swing rotation. SEM top views (left column) and cross-sectional views (right column) of the Si structures grown at $\theta = 85°$ with (a) swing angle $\phi = 45°$ and (b) swing angle $\phi = 75°$. Fanlike structures were still observed. The white scale bar corresponds to a length of 1000 nm. The normal thickness of the deposition was 1000 nm.

a smaller fan-out angle χ compared to the stationary deposition case during the initial stages of growth, as shown in Fig. 6. The incident angle was $\theta = 85°$ in our experiments and the swing angle ϕ was varied for different experiments. The fan-out angle χ depends on the swing angle ϕ. For example, the fan-out angle was measured to be about $54.3 \pm 1.5°$ for the 45° swing angle and about $49.1 \pm 2.7°$ for the 75° swing angle. The reason of the decreasing of the fan-out angle χ with the increased swing angle ϕ is that the deposition flux can cover more surface areas of the structures by swinging to a larger swing angle ϕ. After a short period of deposition, the growth of the width R were observed to have been slowing down in the direction perpendicular to the incident flux because of the global shadowing effects from the adjacent neighbors. Correspondingly, the growth exponent p is expected to be less than 1. Due to the global shadowing, a uniform size rodlike structure can be obtained after the width R reaches a maximum value R_{max}, as shown in Fig. 7. R_{max} is dependent on the swing angle ϕ. The swing angle was set to 90° for the deposition of well separated nanorods as depicted in Fig. 7. The tilted angle of the Si structures was measured to be $56.6 \pm 0.4°$ from Fig. 7(b).

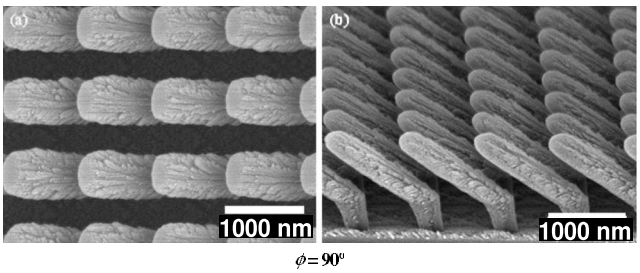

FIG. 7. (a) SEM top view and (b) cross-sectional view of uniform slanted Si structures on seeds (tungsten pillars) by swing rotation at $\theta = 85°$ and swing angle $\phi = 90°$. The structures maintain a uniform width after the initial stage of growth.

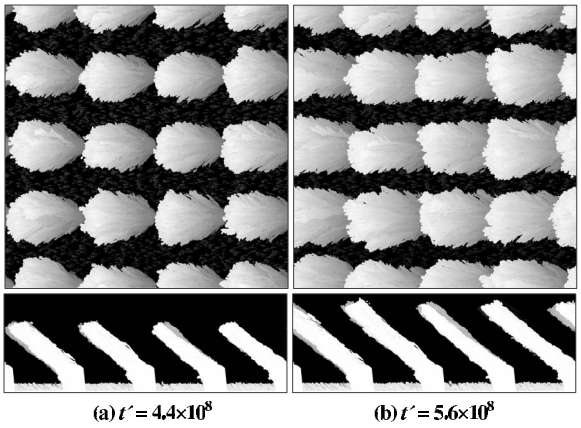

FIG. 8. Top view and cross-sectional view of the Monte Carlo simulations of swing rotation at $\phi = 90°$ and $\theta = 85°$ for two different simulation time t'. The structures have no significant fan-out in this simulation with the swing rotation.

2. Monte Carlo simulation results

Quantitative analysis of this growth behavior under swing rotation was carried out using Monte Carlo simulations. The size of the simulation system is $1024 \times 1024 \times 1024$. The generated particles approached the system at an angle fixed at 85° with respective to the z direction (the substrate normal). The rotational speed in the simulations was defined by the number of particles deposited in one step of substrate rotation. In our code, we chose the method of changing the azimuthal angle of the incident flux to mimic the substrate swing rotation in our experiment. The azimuthal angle of the incident particles was changed at each simulation step but the maximum angle away from the x direction was fixed at $\phi = 30°$, 60°, 75°, and 90° which are equivalent to the swing angles used in the experiments (as schematically presented in Fig. 1). The step of increasing and decreasing the azimuthal angles is the parameter representing the substrate rotational speed. In this simulation, the rotation speed is fixed at 5000 particles per step. We estimated that this rotation speed is on the order of 0.27 rpm of the substrate rotational speed in our experiment with a deposition rate of 30 ± 2 nm/min. However, the rotational speed should not dramatically change the morphology of the structures, as indicated by our geometrical model of the swing rotation.[27] Surface diffusion was introduced in the simulations with a diffusion strength $D/F = 100$ $(F = 1)$. Figure 8 shows the top view and cross-sectional view of the Monte Carlo simulations at two different stages of deposition with swing angle $\phi = 90°$. From the snapshots, the aggregates on the seeds are well separated with the axis inclines from the z direction (the substrate normal). The tilted angle measured from Figs. 8(a) and 8(b) is $53.5 \pm 0.3°$, which is close to the value of $56.6 \pm 0.4°$ that we measured from our experimental result as shown in Fig. 7(b). The rods are uniform in diameter after the maximum value R_{max} is reached, as shown in the cross-sectional images in the Monte Carlo simulations. The size of the rods only grew at the very beginning and then quickly became saturated at a size of 184 ± 21 lattice units when measured from the top view of the simulated images. We also performed experi-

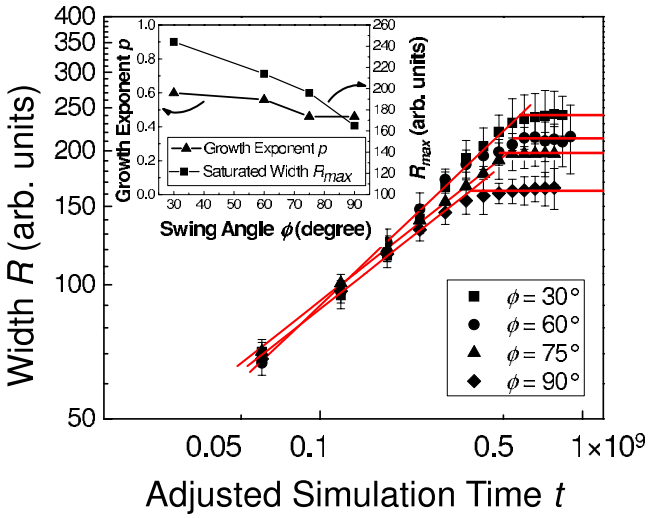

FIG. 9. (Color online) The growth behavior of the aggregates in the Monte Carlo simulations of swing rotation with various swing angles. The width R grows with the simulation time in a power law with the exponent $p<0.6$. The width eventually is saturated at a maximum value R_{max} as indicated by the horizontal solid lines. The inset is the extracted growth exponent p and the maximum width R_{max} for different swing angles from the simulations.

ments and simulations for swing angle $\phi>90°$. Well separated structures without continuously fanning out were also obtained from those experiments and simulations. Hence, we conclude that ballistic fanlike structures are controlled by the substrate swing rotation that provides us an easy way to fabricate identical and well separated nanostructures.

We measured the size of the structures on the seeds generated by the Monte Carlo simulations in the direction perpendicular to the flux (the y direction). The growth of the width R in the y direction was plotted in Fig. 9 as a function of the adjusted simulation time t in log-log scale for various swing angles. The growth exponent p was extracted from this plot following the same method that we used in the previous section. The value of the exponent p was determined as a function of the swing angle ϕ and was <0.6 as shown in the inset of Fig. 9. The width of the aggregates grows with time until reaching a maximum width of R_{max}. The maximum width R_{max} depends on the swing angle ϕ. Specifically, the value of R_{max} decreases as we increase the swing angle. This result is consistent with our experimental observation.[27] From the inset of Fig. 9, both R_{max} and p decrease monotonically with the increase of swing angle ϕ. However, the value of the exponent p maintains a constant value of around 0.46 for swing angle $>75°$. We believe that the reduction of p from 1 (no swing case) to 0.46 is primarily due to the self-shadowing. To verify this, we also performed a simulation using only one single seed to study the effect of self-shadowing on the exponent p, which is similar to the simulation method used by Pelliccione and Lu recently.[31] We observed that the growth exponent p is around 0.5. The global shadowing is not included in this simulation of swing rotation with 85° flux incident angle and 90° swing angle. The structure grown on the single seed has no maximum width R_{max} because there is no global shadowing effect (no adjacent neighbors). Therefore, we believe that the exponent $p\sim0.46$ is dominated by the self-shadowing effect during the substrate swing rotation. Overall, our results reveals that the growth exponent $p\sim1$ due to the NN ballistic sticking and $p\sim0.46$ due to the (geometric) self-shadowing effect.

IV. CONCLUSIONS

In conclusion, we studied the BA of Si particles on arrays of seeds from experiments and simulations with 85° oblique angle incident flux. A fanlike aggregate was observed in experiments and Monte Carlo simulations when the substrate was stationary. We related the growth of the size of the fanlike structures R with the aggregation time t in a power law format $R\sim t^p$. The growth exponent p is ~1 for the stationary deposition in the oblique angle BA simulations with NN sticking and diffusion. The growth exponent $p\sim1$ is consistent with our experimental observations. However, a uniform Si structure can be formed if the substrate is rotated back-and-forth azimuthally within a certain angle. The model used to simulate this substrate swing rotation includes the ballistic NN sticking of particles, surface diffusion, and substrate motion. For faster computation times, a 3D Monte Carlo code was developed to simulate the growth process including these effects. The substrate swing rotation was equivalent to changing the direction of incident flux azimuthally in each cycle of simulation. We estimated the growth exponent $p\sim0.46$ when the substrate motion was included. As a result, uniform aggregates without significant fanlike morphology were generated by the simulations, which is consistent with our experimental results. Therefore, in spite of the complicated nature of oblique angle deposition, our model describes the experimental results reasonably well.

ACKNOWLEDGMENTS

This work is supported by NSF under Grant No. NIRT-0506738. We thank B. K. Lim (Chartered Semiconductor Manufacturing, Singapore) for providing us with the tungsten seeds. We thank G.-C. Wang of Rensselaer Polytechnic Institute and Mark Choyce of the Clarkson University (Potsdam, NY) for valuable suggestions. Mark Choyce worked with us as a summer student in 2006 under the NSF-REU program.

*yed@rpi.edu

[1] A.-L. Barabasi and H. E. Stanley, *Fractal Concepts in Surface Growth* (Cambridge University Press, New York, NY, 1995).
[2] T. Viscek, *Fractal Growth Phenomena* (World Scientific Publishing, Singapore, 1989).
[3] E. Ben-Jacob and P. Garik, Nature (London) **343**, 523 (1990).
[4] T. A. Witten and L. M. Sander, Phys. Rev. Lett. **47**, 1400 (1981); Phys. Rev. B **27**, 5686 (1983).
[5] M. T. Vold, J. Colloid Sci. **18**, 684 (1963); D. N. Sutherland, J. Colloid Interface Sci. **22**, 300 (1966); **25**, 373 (1967).
[6] R. C. Ball and T. A. Witten, Phys. Rev. A **29**, 2966 (1984); J. Stat. Phys. **36**, 873 (1984).
[7] P. Meakin, J. Phys. A **18**, L661 (1985); J. Colloid Interface Sci. **105**, 240 (1985).
[8] F. Family and T. Viscek, J. Phys. A **18**, 75 (1985).
[9] S. Liang and L. P. Kadanoff, Phys. Rev. A **31**, 2628 (1985).
[10] D. Bensimon, B. Shraiman, and S. Liang, Phys. Lett. **102A**, 238 (1984).
[11] P. Ramanlal and L. M. Sander, Phys. Rev. Lett. **54**, 1828 (1985).
[12] A. V. Limaye and R. E. Amritkar, Phys. Rev. A **34**, 5085 (1986).
[13] F. Porcu and F. Prodi, Phys. Rev. A **44**, 8313 (1991).
[14] J. Krug and P. Meakin, Phys. Rev. A **43**, 900 (1991).
[15] V. Singh, in *Handbook of Thin-Film Deposition Processes and Techniques—Principles, Methods, Equipment and Applications*, 2nd ed., edited by K. Seshan (Noyes Publications/William Andrew Publishing, Norwick, NY, 2002), Chap. 5.
[16] D.-X. Ye and T.-M. Lu, Phys. Rev. B **75**, 115420 (2007).
[17] J. M. Nieuwenheuzen and H. B. Haanstra, Philips Tech. Rev. **27**, 87 (1966).
[18] H. J. Leamy, G. M. Gilmer, and A. G. Dirks, Curr. Top. Mater. Sci. **6**, 309 (1980).
[19] L. Ablemann and C. Lodder, Thin Solid Films **305**, 1 (1997).
[20] A. G. Dirks and H. J. Leamy, Thin Solid Films **47**, 219 (1977).
[21] N. G. Nakhodkin and A. I. Shaldervan, Thin Solid Films **10**, 109 (1972).
[22] T. Hashimoto, K. Okamoto, K. Hara, M. Kamiya, and H. Fujiwara, Thin Solid Films **91**, 145 (1982).
[23] O. Geszti, L. Gosztola, and E. Seyfried, Thin Solid Films **136**, L35 (1986).
[24] R. N. Trait, T. Smy, and M. J. Brett, Thin Solid Films **226**, 196 (1993).
[25] F. Tang, D.-L. Liu, D.-X. Ye, Y.-P. Zhao, T.-M. Lu, G.-C. Wang, and A. Vijayaraghavan, J. Appl. Phys. **93**, 4194 (2003).
[26] S.-N. Mei and T.-M. Lu, J. Vac. Sci. Technol. A **6**, 9 (1988).
[27] D.-X. Ye, T. Karabacak, R. C. Picu, G.-C. Wang, and T.-M. Lu, Nanotechnology **16**, 1717 (2005).
[28] K. Robbie, M. J. Brett, and A. Lakhtakia, Nature (London) **384**, 616 (1996).
[29] K. Robbie, J. C. Sit, and M. J. Brett, J. Vac. Sci. Technol. B **16**, 1115 (1998).
[30] Y.-P. Zhao, D.-X. Ye, G.-C. Wang, and T.-M. Lu, Nano Lett. **2**, 351 (2002).
[31] M. Pelliccione and T.-M. Lu, Phys. Rev. B **75**, 245431 (2007).